Simulation of the Two-Area Deregulated Power System using Particle Swarm Optimization

D. Lakshmi[1], A. Peer Fathima[2] and Ranganath Muthu[3]

[1]Dept of EEE, Sree Sastha Institute of Engineering and Technology, Chennai, India. [2]School of Electrical Engineering, VIT University Chennai Campus, India [3]Dept of EEE SSN College of Engineering, Chennai, India
lakshmiee@gmail.com, Peerfathima.a@vit.ac.in, ranganathm@ssn.edu.in

Abstract: In the power system operation, the Load Frequency Control (LFC) is required for good quality reliable electric power supply. The main aim of the load frequency control is to maintain the frequency of each area and the tie-line power flow within the specified tolerance. This is achieved by adjusting the real power output of the generators for the corresponding changes in the load demand. Electric power industry is now an open market structure. This deregulated environment comprises of GENCOs, TRANSCOs and DISCOs, which are supervised by an Independent Service Operator (ISO). In this paper, the transaction between the GENCOs and DISCOs in the deregulated market structure based on the DISCO Participation Matrix (DPM) is designed and simulated. The Proportional-Integral (PI) controller is used to tune the LFC. In this tuning, an intelligent global Particle Swarm optimization (PSO) algorithm is used, which is a population based evolutionary algorithm. The dynamic response of the system is improved by minimizing the Integral Square Error (ISE). The response of the PSO tuned PI controller is compared with the response of the conventional PI controller for the system considered. It is found that, the response of the proposed PSO tuned PI controller is better than that of the conventional PI controller. The simulation is implemented in MATLAB-Simulink.

Keywords: Load Frequency Control, Deregulation, Frequency Regulation, Bilateral Market structure, DISCO Participation Matrix, ACE Participation factor, Proportional Integral controller, Particle Swarm Optimization, Integral Square Error.

1. Nomenclature

LFC	-	Load Frequency Control
ACE	-	Area Control Error
cpf	-	Contract Participation Factor
DPM	-	DISCO Participation Matrix
DISCOs	-	Distribution companies
GENCOs	-	Generation companies
APF	-	ACE Participation Factor
ISE	-	Integral Square Error
R	-	Speed Regulation of Governor
T_G	-	Time Constant of Governor
T_T	-	Time constant of a non-reheat steam turbine
T_P	-	Time constant of power system
K_P	-	Gain constant of power system
B	-	Bias factor
ΔP_{tie}	-	Tie line power flow
Δf	-	Change in frequency
ΔX_E	-	Change in Governor valve position
ΔP_G	-	Change in mechanical turbine output

Received: November 28th, 2014. Accepted: February 10th, 2016
DOI: 10.15676/ijeei.2016.8.1.7

2. Introduction

The good quality of power supply requires the maintenance of frequency and voltage within the tolerable limits, i.e. the main objective of power system operation and control is to provide a balance between the generation and the load. For better performance of the system and to meet the demand, two or more areas are interconnected through a tie-line. The load variation in an area varies affects the remaining areas, which will reflect as changes in frequency (real power), and voltage (reactive power).

Regulation of the real power is achieved by Load frequency Control (LFC) whereas the regulation of the reactive power is achieved by Automatic Voltage Regulator (AVR). In this work, as we are considering the real power output of the generating unit (or frequency). The LFC maintains the desired output frequency and the tie-line power flow. The concept of LFC in a vertically integrated power system was discussed by Elgerd [1] - [3].

Vertical Integrated Utility (VIU) has its own generation-transmission-distribution systems that supply power to the customer. VIU is the sole authority to fix the price of electric energy. Thus, electric power can be bought and sold as a monopoly, along the tie-lines. Moreover, such interconnection provides greater reliability.

The merits and demerits of various controllers used for the LFC for VIU are discussed in [4]. Several control strategies were used to control the frequency and to maintain the scheduled tie-line power flow. The integral action in the PI controller reduces the steady state error to zero. However, this action offers poor dynamic response under variable loads. Conventional PI controllers are tuned using trial and error method and the Ziegler-Nichol's method. Many artificial intelligence based robust controllers use genetic algorithm and the Tabu search algorithm for tuning the parameters of the PID controller in LFC using performance indices [5], [6].

The electric power industry faces many problems due to the ever-increasing demand of the electrical power. These problems may be solved by adopting a deregulated structure, which can improve the efficiency and quality of operation of the power system. Under the deregulation environment, the electric utility will try to innovate for improving the service, which in turn saves its costs and maximizes the profit. The primary criteria applied to support deregulation are that a freer market promotes efficiency. Under the deregulated environment, the power system is split into GENCOs (generation companies), TRANSCOs (transmission companies) and DISCOs (Distribution companies) [7], [8].

GENCOs compete among themselves to sell the power they produce. TRANSCOs are accessible to any GENCO or DISCO for wheeling of the power. DISCO may contract individually with a GENCO for power and these transactions are made under the supervision of the Independent System Operator (ISO).

ISO has a control over the transaction via ancillary services and 12 ancillary services are suggested by the NERC (North American Reliability Council) [9]. Among the 12 ancillary services, regulation and load following are the two frequency related ancillary services. The LFC takes care of these two ancillary services and is considered in this work [10] - [12].

Donde et al [13] presented the concept of DPM and ACE Participation Factors (APF) to represent a bilateral structure in the deregulated environment. The gradient Newton algorithm was used to obtain the optimal parameters. An AGC simulator model for price-based operation in a deregulated system was discussed in [14], [15].

The dynamic response of an interconnected power system under an open market scenario with the HVDC link was investigated in [16], [17]. Comparison of the two-area VIU and the deregulated power system with gradient-based iterative controller has been studied in [18]. Optimal tuning of the PID controller by applying hybrid Bacterial Foraging with Particle Swarm Optimization (BF-PSO) was carried out and the same was compared with I, ID and PI, with the hybrid BF-PSO proving to be better [19].

In this paper, the two-area deregulated market structure is considered. The concept of Disco Participation Matrix (DPM) is implemented. Simulation under various normal operating

conditions and contract violation is carried out for the conventional (PI) controller and the PSO tuned controller. Simulation results show that PSO-PI is better.

The paper is structured as follows; Section 3 explains the deregulated power system in detail. Section 4 represents the DPM, block diagram and state space variables. Section 5 deals with the conventional PI controller and the PSO tuned PI controller, and the design of PSO-PI controller for the deregulated structure. Section 6 presents the case studies, simulation results and the results obtained from the controllers are compared. The conclusion of the work and future line of the research is given in Section 7.

3. Deregulated Power System

The deregulated power system has many GENCOs and DISCOs. A DISCO can have a contract with any GENCO for the transaction of power. If a DISCO in one control area has contract with a GENCO in the same area it is called as "Pool–co" transaction and if a DISCO have contract with a GENCO in another control area, this type of transaction is called as "Bilateral" transaction, which is cleared by the ISO.

4. Formation of The Deregulated Power System

A. DISCO Participation Matrix

The concept of the DISCO Participation Matrix (DPM) is used to visualize the contracts done between a DISCO and a GENCO. The DPM is a matrix in which the number of rows equal to the number of GENCOs and the number of columns equal to the number of DISCOs of the system. The matrix entries are called as the contract participation factor, i.e. the fraction of the total contract by a DISCO (column) with a GENCO (row). Equation 1 gives the DPM for the power system, where 'ijth' entry of the matrix represents the fraction of the total contract by the DISCO 'j' with a GENCO'i' and the sum of all the entries in a particular column is unity. In this paper, a sample system chosen for study is given Figure 1. It is assumed that all the two areas are identical and each area has two GENCOs and two DISCOs and the DPM is given in equation 1 [13],

$$\text{DPM} = \begin{array}{c} \\ \text{No of DISCOs} \end{array} \overset{\text{No of GENCOs}}{\begin{bmatrix} cpf_{11} & cpf_{12} & cpf_{13} & cpf_{14} \\ cpf_{21} & cpf_{22} & cpf_{23} & cpf_{24} \\ cpf_{31} & cpf_{32} & cpf_{33} & cpf_{34} \\ cpf_{41} & cpf_{42} & cpf_{43} & cpf_{44} \end{bmatrix}} \quad \text{with} \quad \sum cpf_{ij} = 1 \tag{1}$$

$$\text{where, } \text{cpf}_{ij}^{..} = \frac{\text{Demand of DISCO 'j' from GENCO 'i'}}{\text{Total Demand of DISCO 'j'}}$$

B. Block Diagram Representation

As there are many GENCOs in each area, ACE has to be distributed among them in proportion to their participation in the LFC. The elements that contribute ACE to the participating GENCOs are represented as ACE Participation Factors (APF). In addition, the summation of the APF in a particular area must be equal to unity as shown in equations 2 and 3.

$$APF_1+APF_2=1 \tag{2}$$
$$APF_3+APF_4=1 \tag{3}$$

When a DISCO demands a specific GENCO or GENCOs for the load, then it must be reflected in the system dynamics i.e. the turbine and governor units should respond. Hence, a particular set of GENCO is supposed to follow the load demanded by a DISCO, as in Equation 1.

Figure 1 shows the block diagram of the two-area deregulated power system in which each area consists of two GENCOs and two DISCOs connected by a tie-line. The transfer function model of the power system considered is shown in Figure 2, which consists of two non-reheat thermal units as the two GENCOs in each area and interconnected by a tie line. The values of the gain and time constants and rating of the system used are given in the Appendix and the symbols used were represented in nomenclature.

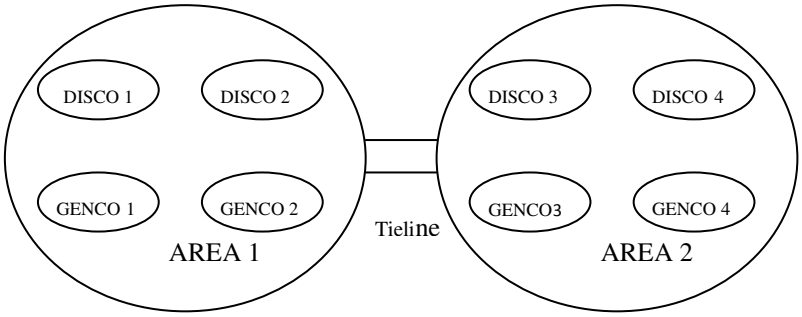

Figure 1. Schematic diagram of a two-area bilateral system

From Figure 2, the contracts were ΔP_1, ΔP_2, ΔP_3, ΔP_4, $\Delta PL_{1,Loc}$ and $\Delta P_{L2,Loc}$. Under steady state, the contract of the DISCOs with GENCOs are shown in equations 4-9,

$$\Delta P_{L1,Loc} = \Delta P_{L1} + \Delta P_{L2} \quad (4)$$
$$\Delta P_{L2,Loc} = \Delta P_{L3} + \Delta P_{L4} \quad (5)$$
$$\Delta P_1 = cpf_{11}\ \Delta P_{L1} + cpf_{12}\ \Delta P_{L2} + cpf_{13}\ \Delta P_{L3} + cpf_{14}\ \Delta P_{L4,} \quad (6)$$
$$\Delta P_2 = cpf_{21}\ \Delta P_{L1} + cpf_{22}\ \Delta P_{L2} + cpf_{23}\ \Delta P_{L3} + cpf_{24}\ \Delta P_{L4} \quad (7)$$
$$\Delta P_3 = cpf_{31}\ \Delta P_{L1} + cpf_{32}\ \Delta P_{L2} + cpf_{33}\ \Delta P_{L3} + cpf_{34}\ \Delta P_{L4} \quad (8)$$
$$\Delta P_4 = cpf_{41}\ \Delta P_{L1} + cpf_{42}\ \Delta P_{L2} + cpf_{43}\ \Delta P_{L3} + cpf_{44}\ \Delta P_{L4.} \quad (9)$$

where, ΔP_{UC1} and ΔP_{UC2} are used for the uncontracted loads and when the uncontracted loads are absent, then $\Delta P_{UC1} = \Delta P_{UC2} = 0$.

The scheduled steady state power flow on the tie-line from area 1 to area 2 is the difference between the demand of DISCOs in the area 2 and GENCOs in the area 1 and the difference between the demand of the DISCOs in area 1 from the GENCOs in area 2, as given by Equation 10,

$$\Delta P_{tie1,2schedule} = \sum_{i=1}^{2}\sum_{j=3}^{4} cpf_{ij}\Delta P_{Lj} - \sum_{i=3}^{4}\sum_{j=1}^{2} cpf_{ij}\Delta P_{Lj} \quad (10)$$

The actual power flow on the tie-line from area 1 to area 2 is the product of the tie-line coefficient and the difference between the change in frequency in area 1 and the change in frequency in area 2, as given by Equation 11,

$$\Delta P_{tie12actual} = \frac{2\Pi T_{12}}{s}\left[\Delta f_1 - \Delta f_2\right] \quad (11)$$

Equation 11 shows the scheduled tie-line power flow

$$\Delta P_{tie1,2\ schedule} = (cpf_{13}+cpf_{23})\Delta P_{L3}+(cpf_{14}+cpf_{24})\Delta P_{L4} - (cpf_{31}+cpf_{41})\Delta P_{L1}-(cpf_{32}+cpf_{42})\Delta P_{L2} \quad (12)$$

Equation 13 gives the error in the tie-line power flow from area 1 to area 2, which is the difference between the actual and scheduled value of the tie-line power.

$$\Delta P_{tie12error} = \Delta P_{tie12actual} - \Delta P_{tie12schedule} \tag{13}$$

Equation 14 gives the error in the tie-line power flow from area 2 to area1.

$$\Delta P_{tie21error} = a_{12}\, \Delta P_{tie12error} \tag{14}$$

Since area 1 is identical to area 2, $a_{12} = -1$

Equation 15 gives the Area Control Error (ACE) of area 1, which is the summation of the bias factor, the deviation of the frequency and the change in tie-line power flows. Similarly, Equation 16 gives the ACE of area 2.

$$ACE_1 = B_1 \Delta f_1 + \Delta P_{tie12error} \tag{15}$$

$$ACE_2 = B_2 \Delta f_2 + a_{12} \Delta P_{tie12error} \tag{16}$$

C. State Space Representation of The Two Area Bilateral Structure

Equation 17 characterizes the state space representation of the closed loop system shown in Figure 2,

$$\dot{X} = AX + BU + CP_d \tag{17}$$

where X is the state vector, U is the control vector, P_d is the demand of the DISCOs and A, B and C are the matrices The state variable vector X has 13 variables. They are (i) change in frequency in each area (Δf_1 and Δf_2), change in Governor valve position in each area (ΔX_{E1} and ΔX_{E2}), change in mechanical turbine outputs in each area (ΔP_{G1} and ΔP_{G2}), integral of ACE in each area ($\int ACE_1 dt$ and $\int ACE_2 dt$) and change in tie line power ($\Delta ptie_{12}$).

The state matrices are presented as follows

$$X = \left[\Delta f_1 \;\; \Delta f_2 \;\; \Delta P_{G1} \;\; \Delta X_{E1} \;\; \Delta P_{G2} \;\; \Delta X_{E2} \;\; \Delta P_{G3} \;\; \Delta X_{E3} \;\; \Delta P_{G4} \;\; \Delta X_{E4} \;\; \Delta P_{tie12} \;\; \int ACE_1 dt \;\; \int ACE_2 dt\right]^T$$

$$A = \begin{bmatrix}
-1/T_{P1} & 0 & 0 & 0 & 0 & 0 & 0 & 0 & 0 & 0 & -K_{P1}/T_{P1} & 0 & 0 \\
0 & -1/T_{P1} & 0 & 0 & 0 & 0 & 0 & 0 & 0 & 0 & -a_{12}K_{P2}/T_{P2} & 0 & 0 \\
0 & 0 & -1/T_{T1} & 1/T_{T1} & 0 & 0 & 0 & 0 & 0 & 0 & 0 & 0 & 0 \\
-1/R_1T_{G1} & 0 & 0 & -1/T_{G1} & 0 & 0 & 0 & 0 & 0 & 0 & 0 & 0 & 0 \\
0 & 0 & 0 & 0 & -1/T_{T2} & 1/T_{T2} & 0 & 0 & 0 & 0 & 0 & 0 & 0 \\
-1/R_2T_{G2} & 0 & 0 & 0 & 0 & -1/T_{G2} & 0 & 0 & 0 & 0 & 0 & 0 & 0 \\
0 & 0 & 0 & 0 & 0 & 0 & -1/T_{T3} & 1/T_{T3} & 0 & 0 & 0 & 0 & 0 \\
0 & -1/R_3T_{G3} & 0 & 0 & 0 & 0 & 0 & -1/T_{G3} & 0 & 0 & 0 & 0 & 0 \\
0 & 0 & 0 & 0 & 0 & 0 & 0 & 0 & -1/T_{T4} & 1/T_{T4} & 0 & 0 & 0 \\
0 & -1/R_4T_{G4} & 0 & 0 & 0 & 0 & 0 & 0 & 0 & -1/T_{G4} & 0 & 0 & 0 \\
2\prod/T_{12} & -2\prod/T_{12} & 0 & 0 & 0 & 0 & 0 & 0 & 0 & 0 & 0 & 0 & 0 \\
B_1 & 0 & 0 & 0 & 0 & 0 & 0 & 0 & 0 & 0 & 1 & 0 & 0 \\
0 & B_2 & 0 & 0 & 0 & 0 & 0 & 0 & 0 & 0 & a_{12} & 0 & 0
\end{bmatrix}$$

$$B = \begin{bmatrix} 0 & 0 \\ 0 & 0 \\ 0 & 0 \\ apf_1 / T_{G1} & 0 \\ 0 & 0 \\ apf_2 / T_{G2} & 0 \\ 0 & 0 \\ 0 & apf_3 / T_{G3} \\ 0 & 0 \\ 0 & apf_4 / T_{G4} \\ 0 & 0 \\ 0 & 0 \\ 0 & 0 \end{bmatrix} \qquad U = \begin{bmatrix} \Delta P_{C1} \\ \Delta P_{C2} \end{bmatrix} \qquad P_d = \begin{bmatrix} P_{L1} \\ P_{L2} \\ P_{L3} \\ P_{L4} \\ P_{UC1} \\ P_{UC2} \end{bmatrix}$$

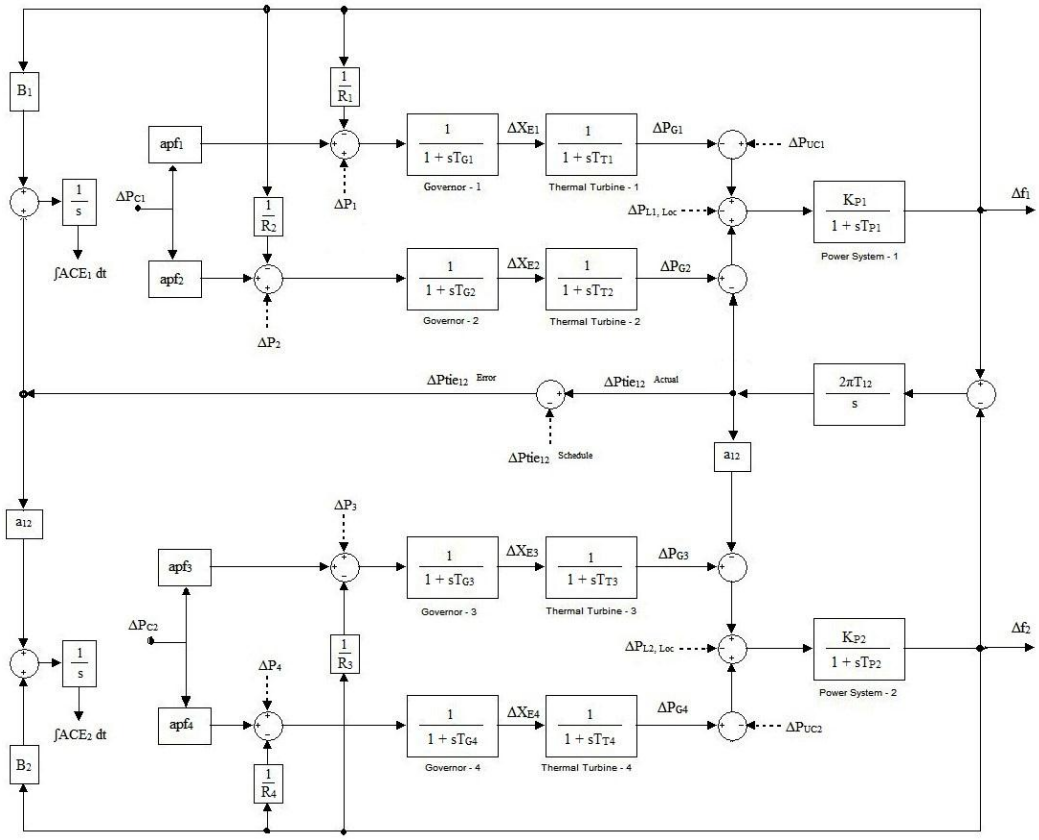

Figure 2. Transfer Function model of a two area deregulated market structure

$$C = \begin{bmatrix} -K_{P1}/T_{P1} & -K_{P1}/T_{P1} & 0 & 0 & -K_{P1}/T_{P1} & 0 \\ 0 & 0 & -K_{P2}/T_{P2} & -K_{P2}/T_{P2} & 0 & K_{P2}/T_{P2} \\ 0 & 0 & 0 & 0 & 0 & 0 \\ cpf_{11}/T_{G1} & cpf_{12}/T_{G1} & cpf_{13}/T_{G1} & cpf_{14}/T_{G1} & 0 & 0 \\ 0 & 0 & 0 & 0 & 0 & 0 \\ cpf_{21}/T_{G2} & cpf_{22}/T_{G2} & cpf_{23}/T_{G2} & cpf_{24}/T_{G2} & 0 & 0 \\ 0 & 0 & 0 & 0 & 0 & 0 \\ cpf_{31}/T_{G3} & cpf_{32}/T_{G3} & cpf_{33}/T_{G3} & cpf_{34}/T_{G3} & 0 & 0 \\ 0 & 0 & 0 & 0 & 0 & 0 \\ cpf_{41}/T_{G4} & cpf_{42}/T_{G4} & cpf_{43}/T_{G4} & cpf_{44}/T_{G4} & 0 & 0 \\ 0 & 0 & 0 & 0 & 0 & 0 \\ (cpf_{31}+cpf_{41}) & (cpf_{32}+cpf_{42}) & -(cpf_{13}+cpf_{23}) & -(cpf_{14}+cpf_{24}) & 0 & 0 \\ a_{12}(cpf_{31}+cpf_{41}) & a_{12}(cpf_{32}+cpf_{42}) & -a_{12}(cpf_{13}+cpf_{23}) & -a_{12}(cpf_{14}+cpf_{24}) & 0 & 0 \end{bmatrix}$$

5. Controllers for The Deregulated Power System

A. Conventional Controller

Conventional controllers are linear controller, as they work on the fixed parameters values. These controllers have been used for a wide range of systems for the last six decades, all around the world. These are the Proportional (P) controller, the Proportional Integral (PI) controller and the Proportional Integral Derivative (PID) controller. Among these controllers, the PI controller is the highly preferred one. A PI controller is a feedback controller which drives the plant to be controlled by a weighted sum of the error (difference between the output and the desired set-point) and the integral of that error.

The inputs to the PI controller for the two-area bilateral market structure are the ACE of the respective areas. Equation 18 expresses the controller output U_{PI},

$$U_{PI} = K_P ACE_i + K_i \int_0^t ACE_i dt \tag{18}$$

where, the controller parameters are K_p, the proportional gain and K_i, the integral gain.

B. Particle Swarm Optimization

PSO was first developed in 1995 by Kennedy and Eberhart. It is a robust stochastic optimization technique based on the movement and intelligence of swarms. The concept of social interaction in this technique is used for problem solving. It uses a number of agents (particles) that constitute a swarm, moving around in the search space looking for the best solution [20].

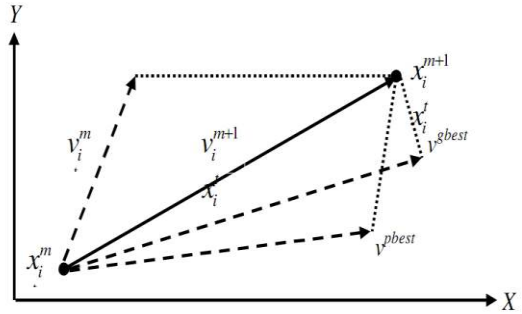

Figure 3. Concept of searching of particles

In this algorithm, each particle is treated as a point in an N-dimensional space which adjusts its "flying" according to its own flying experience as well as the flying experience of other particles based on the flying direction and the distance. Each particle keeps track of its coordinates in the solution space which are associated with the best solution (fitness) that has achieved so far by that particle. This value is called he personal best (*pbest)*. Another best value that is tracked by the PSO is the best value obtained so far by any particle in the neighborhood of that particle. This value is called global best (*gbest)*.Figure 3 shows the concept of searching the particles in search space.

- Velocity Updating

Each particle velocity is updated by Equation 10. The acceleration constants c_1 and c_2 are positive constants known as social parameters, which furnish the right equilibrium between the personal identity and the sociality of the particles, which are taken to be 2. r_1 and r_2 are random numbers between 0 to 1.

$$V_i^{m+1} = V_i^m + c_1 r_1 * (pbest_i - x_i^m) + c_2 r_2 * (gbest - x_i^m) \tag{19}$$

- Position Updating

The position of the particles is updated at each interval, as given by in Equation 11,

$$x_i^{m+1} = x_i^m + V_i^{m+1} \tag{20}$$

whereV_i^m the modified velocity of the particle 'i' at m^{th} iteration. An inertia weight parameter 'w', which deals with the balancing of global search and local search of PSO, is a positive constant lies in between 0.5 to 1. By incorporating these parameters in Equation 19, we achieve the velocity updating given in Equation 21.

$$V_i^{m+1} = w * V_i^m + c_1 r_1 * (pbest_i - x_i^m) + c_2 r_2 * (gbest - x_i^m) \tag{21}$$

C. Design of the PSO-PI Controller

The proper parameters setting makes the system stable. A performance index, which is a quantitative measure of systems, is chosen so that a set of parameters in the system can be adjusted to meet the required specification optimally [21]. Minimum or maximum value of this index corresponds to the optimum set of the parameter value. Equation 22 gives the performance index used to optimize (minimization of the error).

$$ISE = \int_0^\infty e^2(t)dt \tag{22}$$

The PSO algorithm for the system considered has twenty particles. One hundred iterations are chosen for converging. The steps of this algorithm are given below.

Step 1 The error in frequency which is the difference between the set value and the actual value is given as the input to the PSO algorithm, which was obtained from the output of corresponding simulation.

Step 2 Initialize the particles with their random positions and velocities on the N dimensional search space.

Step 3 Initialize loop and each particle, evaluate the desired optimization fitness function in N variables.

Step 4 Calculate and compare the fitness value with its p_{best}. If the current value is better than the p_{best}, then assign p_{best} equal to the current value and p_i equal to present location S_i.

Step 5 Check for the velocity V of each particle according to Equation 23.

$$V_i^{m+1} \geq V_{\max}, then V_i^{m+1} = V_{\max} \tag{23}$$

Step 6 Check the particle in the neighborhood with the best value so far and assign the coordinates of the best particle as g_{best}.
Step 7 Update the velocity of each particle using Equation 20.
Step 8 Update the position of each particle using Equation 21.
Step 9 If the maximum number of iterations is reached, go to the next step otherwise go to step 4.
Step 10 The values of g_{best} obtained are the optimal values of the performance index (optimal values of K_P and K_I of the controller).
Step 11 Stop evaluation procedure.

6. Case Studies and Simulation Results

Simulation was carried out in MATLAB-Simulink for the block diagram shown in Figure 2. Both the areas are assumed to be identical, i.e. governor-turbine units of both the areas were assumed identical. Three different cases of transactions were considered as follows.

A. *Case 1: (Pool-co transaction)*

In this case, the deregulated system shown in Figure 2 is considered and assumed that the load change occurs only in area 1 and GENCOs in this area equally participates(Pool-co transaction). For this condition, APF are calculated as follows:

$APF_1 = 0.5$, $APF_2 = 1\text{-}0.5$,

$APF_3 = 0.5$, $APF_4 = 1\text{-}0.5$ which satisfies $\sum APF_{ij} = 1$

Since $DISCO_3$ and $DISCO_4$ does not demand power from any GENCOs, The corresponding 'cpf' is zero. The 'cpf' for area1 alone is calculated below and DPM matrix is formulated.

$Cpf_{11}=0.05/0.1 = 0.5$, $Cpf_{12}=0.05/0.1 = 0.5$, $Cpf_{21}=0.05/0.1 = 0.5$ and $Cpf_{22}=0.05/0.1 = 0.5$

$$DPM = \begin{bmatrix} 0.5 & 0.5 & 0 & 0 \\ 0.5 & 0.5 & 0 & 0 \\ 0 & 0 & 0 & 0 \\ 0 & 0 & 0 & 0 \end{bmatrix}$$

and the demand of DISCOs in (pu MW) is as follows:

$\Delta P_{L1} = 0.1$, $\Delta P_{L2} = 0.1$, $\Delta P_{L3} = 0$, $\Delta P_{L4} = 0$.

Since the uncontracted load is taken to be zero, $\Delta P_{UC1} = 0$, $\Delta P_{UC2} = 0$ and $P_{tie1,2\ schedule} = 0$ as per equation 12.

Figure ures 4 (a), 4 (b) & 4 (c) shows the comparison of PI and PSO tuned controller dynamic responses of areas 1 and 2 and the tie-line power flow for the case. From Figure 4 it is observed that the settling time, overshoot and undershoot are reduced when compared to the PI controller. Table 1 compares the settling time, overshoot and undershoot for the two controllers.

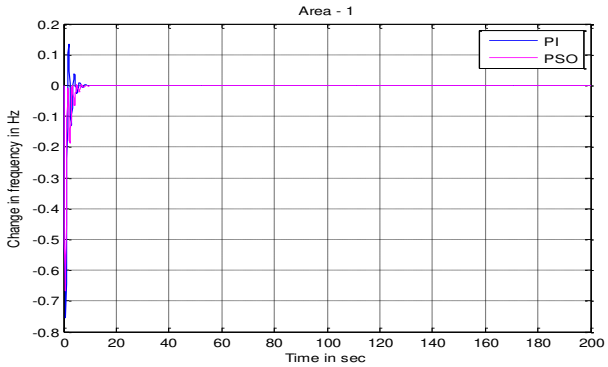

(a)

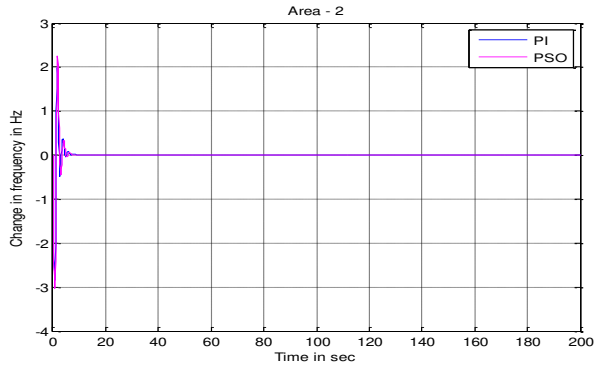

(b)

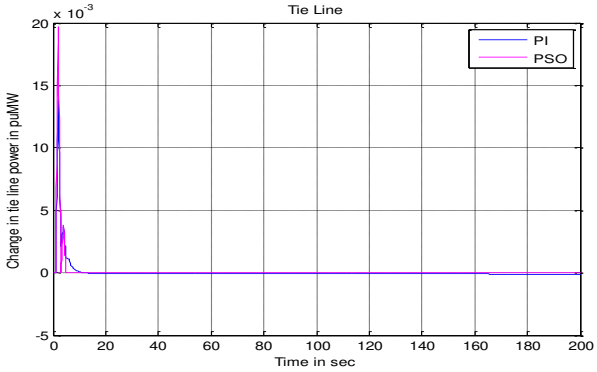

(c)

Figure 4 (a), (b) & (c) dynamic responses of area 1, area 2 and tie-line power flow for case 1

B. Case 2: (Bilateral transaction)

All DISCOs contracts with the GENCOs for power(Bilateral transaction) as per the following DPM,

$$\text{DPM} = \begin{bmatrix} 0.5 & 0.25 & 0 & 0.3 \\ 0.2 & 0.25 & 0 & 0 \\ 0 & 0.25 & 1 & 0.7 \\ 0.3 & 0.25 & 0 & 0 \end{bmatrix}$$

and the corresponding ACE participation factor is as follows: APF_1=0.75, APF_2 = 1-0.75, APF_3 = 0.5 and APF_4=1-0.5. The demand of DISCOs in (pu MW) is ΔP_{L1} = 0.1, ΔP_{L2} = 0.1, ΔP_{L3} = 0, and ΔP_{L4} = 0. Since the uncontracted load is taken to be zero, ΔP_{UC1} = 0, ΔP_{UC2} = 0. Each DISCO demands 0.1 pu MW power from GENCO, as shown by 'cpfs' in DPM matrix. Here the uncontracted load is zero, i.e. no contract violation.As the DISCOs have contract with all GENCOs irrespective of area, this is called as "Bilateral" transaction.

$\Delta P_{tie1,2\ schedule}$ = -0.05 pu MW as per equation 12.

Figure ures 5 (a), 5 (b) & 5 (c) shows the comparison of the PI and the PSO tuned controller dynamic responses of areas 1 & 2 and the tie-line power flow for the case. From Figure 5 it is seen that the settling time, overshoot and undershoot are reduced when compared to the PI controller. Table 1 compares the settling time, overshoot and undershoot for the two controllers.

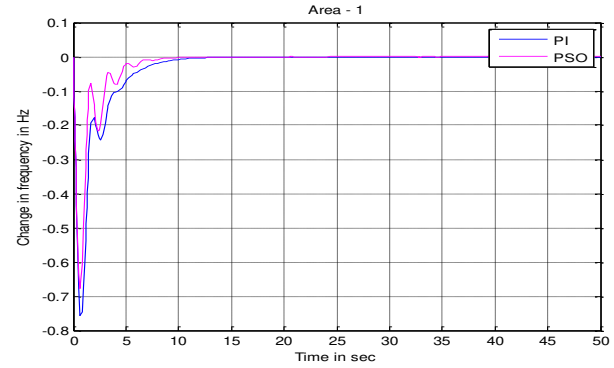

(a)

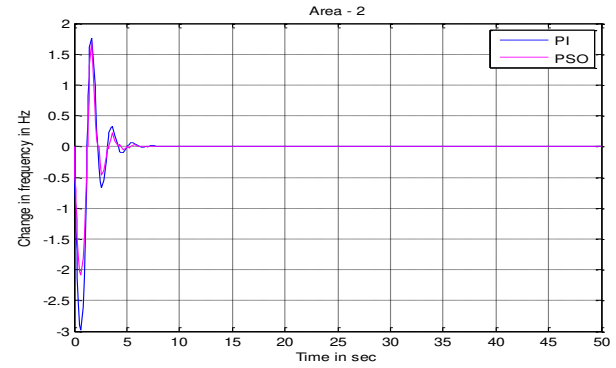

(b)

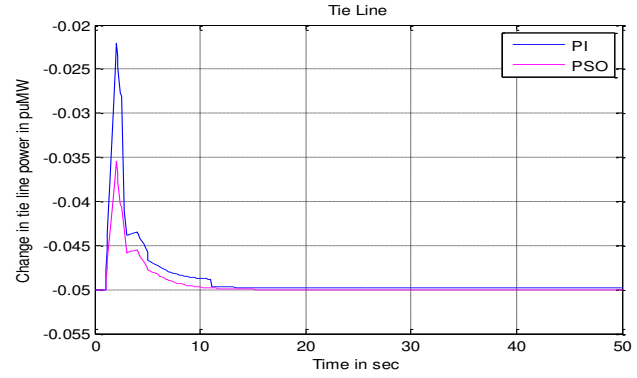

(c)

Figure 5 (a), (b) & (c) dynamic responses of area1, area 2 and tie-line power flow for case 2

C. Case 3 (contract Violation)

Consider a DISCO that violates a contract by demanding more power than specified in the contract. This excess power is not contracted out to any GENCO. This uncontracted power must be supplied by the GENCOs in the same area as the DISCO. This must be reflected as a local load of the area, but not as the contract demand.

Consider case 2 with a modification that $DISCO_3$ demands 0.1 pu MW of excess power and the DPM is same as in case 2.

The total local load in area 1 ($\Delta P_{L1,\,LOC}$) = Load of $DISCO_1$ +load of $DISOC_2$

= 0.1+0.1 pu MW = 0.2 pu MW (no uncontracted load)

Similarly, the total local load in area 2 ($\Delta P_{L2, LOC}$) = Load of $DISCO_3$ +load of $DISOC_4$
= (0.1+0.1) +0.1 pu MW = 0.3 pu MW

The uncontracted load of DISCO3 is reflected in the power generation from GENCO3 and GENCO4. The generation of power from GENCO1 and GENCO2 is not affected by the excess load, which is being taken care of by ISO. In all the cases it is assumed that each area contains at least one GENCO that participates in LFC, i.e. has a nonzero ' APF'. $\Delta P_{tie1, 2\ schedule}$ = -0.05 pu MW as per equation 12 same as in case 2.

Figure ures 6 (a), 6 (b) & 6 (c) show the comparison of the PI and the PSO tuned controller dynamic responses of areas 1 & 2 and the tie-line power flow for case. From Figure 6 it is seen that the settling time, overshoot and undershoot are reduced when compared to the PI controller. Table 1 compares the settling time, overshoot and undershoot for the two controllers.

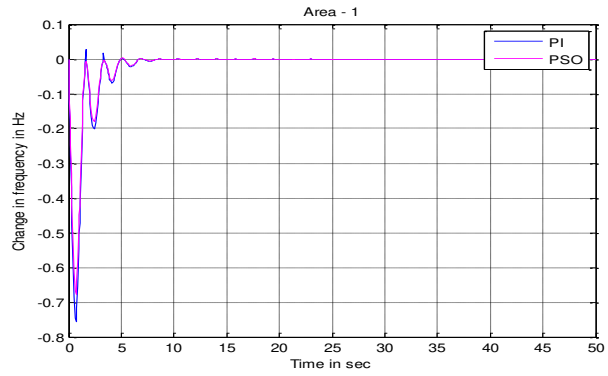

(a)

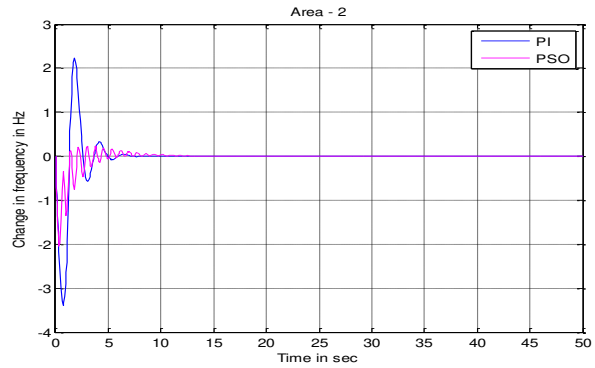

(b)

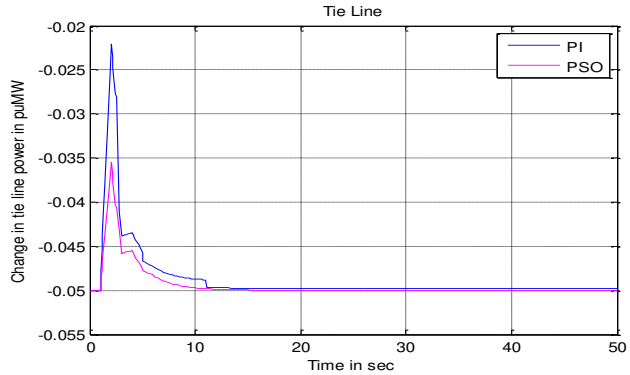

Figure 6 (a), (b) & (c) dynamic responses of area1, area2 and tie-line power flow for case 3

Table 1 compares the response of the conventional PI controller with that of the PSO tuned PI controller for deregulated market structure for two different DPM and contract violation. In case 1, the settling time of the change in frequency in area 1 for PSO-PI controller is 4.8 s, whereas for the PI controller it is 8.7 s. Similarly, the settling time of the change in frequency in area 2 for the PSO-PI controller is 7.2 s, whereas it is 8.4 s for the PI controller. From table 1 and Figure ures 4, 5 and 6, it is seen that the reduction in settling time is around 50% to 25% for PSO tuned controller than the PI controller. The overshoot and the undershoot obtained from PSO-PI controller gives better performance, i.e. the reduction in peaks when compared to the PI controller. Similarly, for case 2 and case 3 , there is reduction in settling time and peaks of over and undershoot occurs for PSO tuned PI controller than PI. From table1 is shown that the PSO tuned PI controller gives better response than PI.

Table 1. Comparison of the frequency and tie line responses for the PI controller and the PSO tuned PI controller

Case	Controller	Layout	Settling time (s)	Overshoot	Undershoot
Case 1	PI	Area 1	8.7	0.125 (Hz)	-0.755 (Hz)
		Area 2	8.4	2.0 (Hz)	-2.9 (Hz)
		Tie line	9.8	0.014 (pu MW)	0 (pu MW)
	PSO–PI	Area 1	4.8	0 (Hz)	-0.665 (Hz)
		Area 2	7.2	1.85 (Hz)	0 (Hz)
		Tie line	6	0.011 (pu MW)	0 (pu MW)
Case 2	PI	Area 1	13	0 (Hz)	-0.75 (Hz)
		Area 2	13	1.8 (Hz)	-3 (Hz)
		Tie line	13	0 (pu MW)	-0.022 (pu MW)
	PSO–PI	Area 1	9	0 (Hz)	-0.67 (Hz)
		Area 2	7	1.6 (Hz)	-2.0 (Hz)
		Tie line	9	0 (pu MW)	-0.035 (pu MW)
Case 3	PI	Area 1	11	0.02 (Hz)	-0.75 (Hz)
		Area 2	14	(2.2Hz)	-3.4 (Hz)
		Tie line	15	0 (pu MW)	-0.023 (pu MW)
	PSO–PI	Area 1	7.5	0 (Hz)	-0.6 (Hz)
		Area 2	6.5	0.05 (Hz)	-2 (Hz)
		Tie line	10	0 (pu MW)	-0.036 (pu MW)

7. Conclusion

This paper investigates the performance of the PI and PSO-PI controllers of a deregulated market structure for different transactions and contract violation. The concept of DISCO participation matrix (DPM) is implemented. A comparison of both the controllers shows that PSO tuned PI controller gives better results than the PI controller, namely reduced settling time, lesser overshoot and undershoot for all the cases under study. Performance characteristics in terms of the performance index Integral Square Error reveals that the designed PSO tuned PI controller is a promising control scheme for the solution of LFC problem and therefore it can be used to generate good quality and reliable electric power in the deregulated power systems. The same can be implemented for the multi-area deregulated power system with non-linearities in the thermal unit.

Appendix 1

P_{r1}= P_{r2}= 2000 MW, H_1 = H_2 = 5 s, D_1 = D_2 = $8.33*10^{-3}$ p.u.MW/Hz, R_1=R_2=R_3=R_4 = 2.4Hz/p.u. MW, K_{P1} = K_{P2} = 120 Hz/p.u. MW, T_{P1} = T_{P2} = 20 s, T_{G1} = T_{G2} = T_{G3} = T_{G4} = 0.08 s, T_{T1}=T_{T2} = 0.3 s, T_{12}= 0.086 s, B_1 = B_2 = 0.425Hz, f = 60Hz, a_{12} = -1.

8. References

[1]. Elgerd O I and Charles Fosha E, "Optimum Megawatt- Frequency Control of Multi area Electric Energy Systems", *IEEE Transactions on Power Apparatus and Systems*, vol. PAS-89, No 4, April 1970, pp. 556-563.

[2]. Elgerd O I, "Electric Energy Systems Theory: An Introduction", New York: McGraw-Hill, 1982.

[3]. Wood A J and Woolen Berg BF, "Power Generation Operation and Control", John Wiley and Sons, 1984.

[4]. Shayeghi H, Jalili A and Shayanfar H A, "Load Frequency Control Strategies: A State of-the-art survey for the researcher", *Energy Conversion and Management* (Elsevier) 50 (2009), pp. 344-353.

[5]. Bassi S J, Mishra M K and Omizegba E E, "Automatic Tuning of Proportional Integral – Derivative (PID) Controller using Particle Swarm Optimization (PSO) Algorithm", *International Journal of Artificial Intelligence & Applications (IJAIA)*, Vol. 2, No.4, October 2011, pp. 25-34.

[6]. Ibraheem and Singh O, "Design of particle swarm optimization (PSO) based automatic generation control (AGC) regulator with different cost functions", *Journal of Electrical and Electronics Engineering Research*, vol. 4(2), November 2012, pp. 33-45.

[7]. Jain S K, Chakrabarti S and Singh S N, "Review of Load Frequency Control Methods, Part-I Introduction and Pre-Deregulation Scenario", *International conference on Control, Automation, Robotics and Embedded Systems (CARE)*", 16th -18th Dec 2013.

[8]. Jain S K, Chakrabarti S and Singh S.N., "Review of Load Frequency Control Methods, Part-II Post-Deregulation Scenario and Case Studies", *International conference on Control, Automation, Robotics and Embedded Systems (CARE)*", 16th -18th Dec 2013.

[9]. Zhong J., "On Some Aspects of Design of Electric Power Ancillary Service Markets", Ph.D. Thesis, Charmers University, Goteberg, Sweden, 2003.

[10]. Christie R D and Bose A, "Load Frequency Control Issues in power system operation after Deregulation", *IEEE Transactions on Power Systems*, vol. 11, No 3, 1996, pp. 191-200.

[11]. Zhao H and Bhattacharya K, "Design of Frequency Regulation Service Market Based on Price and Demand Elasticity Bids", *15th Power System Computation Conference (PSCC), Liege, Belgium*, 22-29, August 2005.

[12]. Peer Fathima A and Abdullah Khan M, "Design of a New Market Structure and Robust Controller for the frequency Regulation Service in the Deregulated Power system", *Electric Power Components and Systems*, vol. 33., No 10, Oct 2008, pp. 864-883.

[13]. Donde V, Pai M A and Hiskens I A, "Simulation and Optimization in an AGC System after Deregulation", *IEEE Transactions on Power Systems*, vol. 16, No 3, Aug 2001, pp.481-489.

[14]. Kumar J, Ng K H and Sheble G, "AGC Simulator for price based operation, Part I: A Model", *IEEE Transactions Power Systems*, vol. 12, No.2, May 1997, pp. 527-532.

[15]. Kumar J, Ng K and Sheble G, "AGC Simulator for price based operation, Part II: Case study Results", *IEEE Transaction on Power Systems*, vol. 12, No.2, May1997, pp. 533-537.

[16]. Srinivasa Rao C., Naghizadeh Z., Mahdavi. S., "Improvement of dynamic performance of hydrothermal system under open market scenario using asynchronous tie-lines", *World Journal of Modelling and Simulation*, vol. 4 (2008) no. 2, pp. 153-160.

[17]. Ibraheem, Prabhat Kumar, Naimul Hasan and Yadav Singh, "Optimal Automatic Generation of Interconnected Power System with Asynchronous Tie-lines under

Deregulated Environment", *Electric Power Components and Systems*, vol. 40, March 2012, pp. 1208-1228.
[18]. Prabhat Kumar, Safia A Kazmi, Nazish Yasmeen, "Comparative study of automatic generation control of traditional and deregulated power environment", *World Journal of Modelling and Simulation*, Vol. 6 (2010), no. 3, pp. 189-197.
[19]. El Yakine Kouba, Menaa M., Hasni M., Boussahoua B and Boudour M., "Optimal Load Frequency Control Based On Hybrid Bacterial Foraging and Particle Swarm Optimization", *Multi –Conference on Systems, Signals & Devices (SSD)*, 2014 11th International date 11-14 Feb,2014.
[20]. Kennedy J, and Eberhart R, "Particle Swarm Optimization", Proceedings of the 1995 IEEE International Conference on Neural Networks, IEEE Press, 1995, pp. 1942-1948.
[21]. Lakshmi D, Peer Fathima A and Ranganath Muthu., "PSO Based Load Frequency Control for Single Area Power System", *International Conference on Electrical, Communication and Computing, ICEEE* – 2014, 13-14 March 2014, pp. 15-19.

D. Lakshmi received her undergraduate degree in Electrical & Electronics Engineering from Madras University in 1999 and postgraduate degree in Power Systems from Anna University in 2006. She is pursuing her Ph.D. from Anna University, Chennai at SSN College of Engineering, India while being an Associate Professor in Department of Electrical & Electronics Engineering at Sree Sastha Institute of Engineering and Technology, Chennai and has been teaching for more than 14 years. Lakshmi has published 10 papers in International Journals and Conference Proceedings and has supervised many undergraduate and postgraduate projects. Her research interests include deregulated power system, power generation & operation, and power system control.

A. Peer Fathima has obtained her B.E degree in Electrical & Electronics Engineering from Madurai Kamaraj University, M.E degree in High voltage Engineering from Anna University, Chennai, and M.S degree in Electronics & Control from BITS Pilani. She received her Ph.D degree from Anna University, Chennai. Currently she is working as a professor in School of Electrical Engineering, VIT Chennai .She has been in the teaching profession for the past 25 years .She has published over 80 papers in International journals / conferences. She has guided several P.G and U.G projects. She is guiding seven Ph.D scholars at Anna and VIT universities. Her main teaching and research interest encompasses power system operation and control in deregulated power systems, renewable energy applications in deregulated power systems.

Ranganath Muthu received his Ph.D. in Control and Instrumentation in 1999. He is a recipientof the Young Scientist Fellowship from Tamil Nadu State Council for Science &Technology, India for 1995-1996. He has more than 25 years of teaching experience and is now a Professor in the Department of Electrical and Electronics Engineering, SSN College ofEngineering, India. He has supervised 7 research scholars for their Ph.D. degree and has published more than 40 papers in technical journals. Dr. Muthu is a Fellow of Institution of Engineers (India), and a senior member of IEEE and ISA. His research interests include intelligent control techniques, power electronics, renewable energy, and advanced control systems.